

Metastable states and quasicycles in a stochastic Wilson-Cowan model of neuronal population dynamics

Paul C. Bressloff

*Mathematical Institute, University of Oxford, 24-29 St. Giles', Oxford OX1 3LB, United Kingdom
and Department of Mathematics, University of Utah, 155 South, 1400 East, Salt Lake City, Utah 84112, USA*
(Received 13 August 2010; revised manuscript received 22 September 2010; published 3 November 2010)

We analyze a stochastic model of neuronal population dynamics with intrinsic noise. In the thermodynamic limit $N \rightarrow \infty$, where N determines the size of each population, the dynamics is described by deterministic Wilson-Cowan equations. On the other hand, for finite N the dynamics is described by a master equation that determines the probability of spiking activity within each population. We first consider a single excitatory population that exhibits bistability in the deterministic limit. The steady-state probability distribution of the stochastic network has maxima at points corresponding to the stable fixed points of the deterministic network; the relative weighting of the two maxima depends on the system size. For large but finite N , we calculate the exponentially small rate of noise-induced transitions between the resulting metastable states using a Wentzel-Kramers-Brillouin (WKB) approximation and matched asymptotic expansions. We then consider a two-population excitatory or inhibitory network that supports limit cycle oscillations. Using a diffusion approximation, we reduce the dynamics to a neural Langevin equation, and show how the intrinsic noise amplifies subthreshold oscillations (quasicycles).

DOI: [10.1103/PhysRevE.82.051903](https://doi.org/10.1103/PhysRevE.82.051903)

PACS number(s): 87.19.lj, 87.19.lc

I. INTRODUCTION

In biochemical and gene networks within cells, there is an important distinction between intrinsic and extrinsic noise [1,2]. Extrinsic noise refers to external sources of randomness associated with environmental factors, and is often modeled as a continuous Markov process based on Langevin equations. On the other hand, intrinsic noise refers to random fluctuations arising from the discrete and probabilistic nature of chemical reactions at the molecular level, which are particularly significant when the number of reacting molecules N is small. Under such circumstances, the traditional approach to modeling chemical reactions based on systems of ordinary differential equations that describe concentration changes via the law of mass action is inappropriate. Instead, a master-equation formulation is necessary in order to describe the underlying jump Markov process. Since master equations are often difficult to analyze, diffusion approximations have been developed for mesoscopic systems (large but finite N) leading to a description based on the chemical Langevin equation [3,4]. Although the diffusion approximation can capture the stochastic dynamics of mesoscopic reacting systems at finite times, it can break down in the limit $t \rightarrow \infty$. For example, suppose that the deterministic system based on the law of mass action (obtained in the thermodynamic limit $N \rightarrow \infty$ for finite t) has multiple stable fixed points. The diffusion approximation can then account for the effects of fluctuations well within the basin of attraction of a locally stable fixed point. However, there is now a small probability that there is a noise-induced transition to the basin of attraction of another fixed point. Since the probability of such a transition is usually of order $e^{-\tau N}$ except close to the boundary of the basin of attraction, such a contribution cannot be analyzed accurately using standard Fokker-Planck (FP) methods [3]. These exponentially small transitions play a crucial role in allowing the network to approach the unique

stationary state (if it exists) in the asymptotic limit $t \rightarrow \infty$. In other words, for multistable chemical systems, the limits $t \rightarrow \infty$ and $N \rightarrow \infty$ do not commute [5–7].

The distinction between intrinsic and extrinsic sources of noise can also be applied to neural systems, both at the single neuron and network levels [8,9]. It is well known that the spike trains of individual cortical neurons *in vivo* tend to be very noisy, having interspike interval distributions that are close to Poisson [10]. The main source of intrinsic fluctuations is channel noise arising from the variability in the opening and closing of a finite number of ion channels. The resulting conductance-based model of a neuron can be formulated as a stochastic hybrid system, in which a continuous deterministic dynamics describing the time evolution of the membrane potential is coupled to a jump Markov process describing channel dynamics [11]. Extrinsic fluctuations at the single cell level are predominantly due to synaptic noise. That is, cortical neurons are bombarded by thousands of synaptic inputs, many of which are not correlated with a meaningful input and can thus be treated as background synaptic noise [9]. It is not straightforward to determine how noise at the single cell level translates into noise at the population or network level. One approach has been developed in terms of a Boltzmannlike kinetic theory of integrate-and-fire networks [12,13], which is itself a dimension reduction by moment closure of the population-density method [14,15]. The latter is a numerical scheme for tracking the probability density of a population of spiking neurons based on solutions of an underlying partial differential equation. In the case of simple neuron models, this can be considerably more efficient than classical Monte Carlo simulations that follow the states of each neuron in the network. On the other hand, as the complexity of the individual neuron model increases, the gain in efficiency of the population density method decreases, and this has motivated the development of moment closure schemes. However, considerable care must be taken when

carrying out the dimension reduction, since it can lead to an ill-posed problem over a wide range of physiological parameters [16]. That is, the truncated moment equations may not support a steady-state solution even though a steady-state probability density exists for the full system.

A number of studies of fully or sparsely connected integrate-and-fire networks have shown that under certain conditions, even though individual neurons exhibit Poisson-like statistics, the neurons fire asynchronously so that the total population activity evolves according to a mean-field rate equation with a characteristic activation or gain function [17–21]. Formally speaking, the asynchronous state only exists in the thermodynamic limit $N \rightarrow \infty$, where N determines the size of the population. This then suggests a possible source of intrinsic noise at the network level arises from fluctuations about the asynchronous state due to finite-size effects [22–25]. (Finite-size effects in IF networks have also been studied using linear-response theory [26–28]). A closer analogy between intrinsic noise in biochemical and neural networks has recently been developed by Bressloff [29] based on a rescaled version of the neural master equation introduced by Buice *et al.* [30,31] (see also [32]). The underlying system consists of a network of coupled homogeneous populations. The state of each population is represented by the number of currently active neurons, and the state transitions are chosen such that deterministic Wilson-Cowan rate equations [33,34] are recovered in the thermodynamic limit $N \rightarrow \infty$. Corrections to the mean-field equations involving higher-order moments can then be obtained by carrying out a Van-Kampen system size expansion along identical lines to chemical master equations [29]; such moment equations can also be obtained by carrying out a loop expansion of a corresponding path-integral representation of the moment generating function [29–31].

In this paper we further develop the connection between chemical and neural master equations, by considering two important effects of intrinsic noise, namely, noise-induced transitions between metastable states, and noise-amplification of subthreshold oscillations or quasicycles. In both cases, we follow along analogous lines to previous studies of biochemical networks. In the case of noise-induced transitions, corrections to mean-field theory based on the system-size or loop expansion break down. Instead, it is more appropriate to analyze the master equation using a Wentzel-Kramers-Brillouin (WKB) approximation and matched asymptotics [5,35–39]. On the other hand, quasicycles can be analyzed by considering the power spectrum of the associated Langevin equation obtained by carrying out a linear noise approximation of the master equation [40,41]. The structure of the paper is as follows. We introduce the birth-death master equation for a single bistable network in Sec. II, and carry out the analysis of noise-induced transitions in Sec. III. In Sec. IV we present the master equation for a multiple population model, and analyze the noise-amplification of subthreshold oscillations in an excitatory or inhibitory network. We also briefly indicate how to extend the analysis of metastability to multiple populations. Finally, in Sec. V we give some possible applications of our analysis.

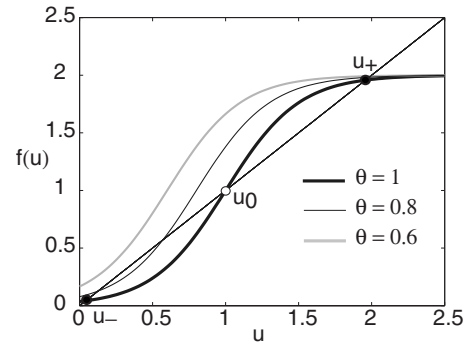


FIG. 1. Bistability in the deterministic network satisfying $\dot{u} = -u + f(u)$ with f given by the sigmoid [Eq. (2.2)] for $\gamma=4$ and $\theta = 1.0$, $f_0=2$. There exist two stable fixed points u_{\pm} separated by an unstable fixed point u_0 . As the threshold θ is reduced the network switches to a monostable regime.

II. MASTER EQUATION FOR A BISTABLE ONE-POPULATION MODEL

Consider a single homogeneous population of excitatory neurons satisfying a simple rate equation of the form

$$\frac{du}{dt} = -\alpha u + f(u), \quad (2.1)$$

where u is a measure of mean population activity, α is a rate constant and f is a nonlinear firing rate function with gain γ and threshold θ . Note that for a single population model, the strength of recurrent connections within the population can be absorbed into the gain γ . For concreteness, f is taken to be the sigmoid function

$$f(u) = \frac{f_0}{1 + e^{-\gamma(u-\theta)}}, \quad (2.2)$$

with f_0 another rate constant. It is straightforward to show graphically that Eq. (2.1) exhibits bistability for a range of values of the gain and threshold. That is, there exist two stable fixed points u_{\pm} separated by an unstable fixed point u_0 (see Fig. 1). We will fix the units of time by setting $\alpha=1$. (We interpret α^{-1} as a membrane time constant such that $\alpha^{-1}=10$ msec in physical units).

We now construct a stochastic version of the above rate model using a master-equation formulation [29–32]. We assume that each neuron can be in either an active or quiescent state. Let $N(t)$ denote the number of active neurons at time t and introduce the probability $P(n, t) = \Pr\{N(t)=n\}$. The latter is taken to evolve according to a birth-death process of the form

$$\begin{aligned} \frac{dP(n, t)}{dt} = & T_+(n-1)P(n-1, t) + T_-(n+1)P(n+1, t) \\ & - [T_+(n) + T_-(n)]P(n, t) \end{aligned} \quad (2.3)$$

for integer $n \geq 0$, with boundary condition $P(-1, t) \equiv 0$ and initial condition $P(n, 0) = \delta_{n, \bar{n}}$. The birth and death rates are chosen to be of the form

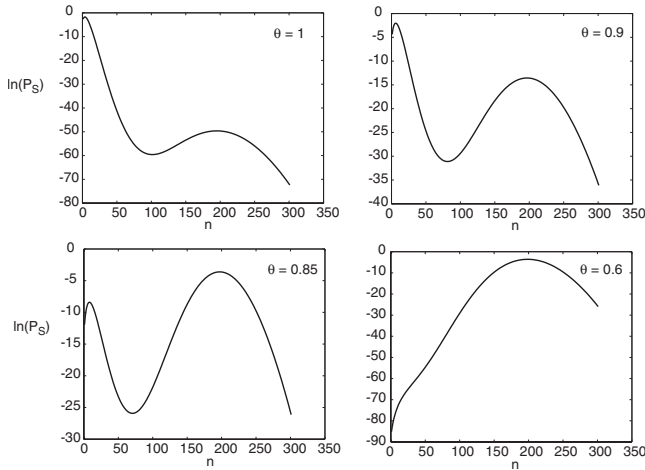


FIG. 2. Plots of the steady-state distribution $P_S(n)$ for various thresholds θ with $\gamma=4.0$ and $f_0=2$. System size is $N=100$.

$$T_+(n) = Nf(n/N), \quad T_-(n) = n, \quad (2.4)$$

where N is a system size parameter such that the deterministic rate Eq. (2.1) is recovered in the thermodynamic limit $N \rightarrow \infty$. That is, multiply both sides of the master Eq. (2.3) by n and sum over n to obtain

$$\frac{d\langle n \rangle}{dt} = \langle T_+(n) \rangle - \langle T_-(n) \rangle, \quad (2.5)$$

where the brackets $\langle \dots \rangle$ denote a time-dependent ensemble averaging over realizations of the stochastic dynamics, that is, $\langle A(n) \rangle = \sum_n P(n, t) A(n)$ for any function of state $A(n)$. We now impose the mean-field approximation $\langle T_{\pm}(n) \rangle \approx T_{\pm}(\langle n \rangle)$, which is based on the assumption that statistical correlations can be neglected in the thermodynamic limit $N \rightarrow \infty$. Identifying mean population activity according to $u = \langle n \rangle / N$ then yields the rate Eq. (2.1). We leave the interpretation of the system size parameter N open here. One possibility would be to identify N with the number of neurons in the population such that $u(t)$ is the mean fraction of active neurons at time t and $0 \leq u \leq 1$. However, N could also be identified with the mean number of synaptic inputs into a neuron in a sparsely coupled network, for example. In this case the number of neurons in the network would be χN for some integer χ , where χ determines the degree of sparseness.

Note that the master Eq. (2.3) is a rescaled version of the one considered by Buice *et al.* [30,31]. That is, they take the

transition rate $T_{\pm}(n) = f(n)$ so that $u = \langle n \rangle$ in the mean-field Eq. (2.1), which corresponds to the mean number of active neurons. Such a choice would be appropriate if population activity were itself Poissonlike, rather than characterized in terms of finite-size fluctuations about an asynchronous state. The advantage of our choice of scaling from an analytical viewpoint is that one can treat N^{-1} as a small parameter and use large deviation theory to study escape from metastable states [35,42,43]. Moreover, the finite time behavior within the basin of attraction of a metastable state can be analyzed using a system size expansion or diffusion approximation [3].

In order to describe the nontrivial effects of fluctuations for large but finite N , suppose that the deterministic network is in the bistable regime so that the system tends toward either the high or low activity stable fixed point as $t \rightarrow \infty$, depending on the initial condition. In the same parameter regime, the stochastic network will also tend toward one of these fixed points on a fast time scale, but will randomly switch between the basins of attraction of the two fixed points on a slower time scale that depends exponentially on the system size N ; the fixed points are thus only metastable in the presence of intrinsic noise. The state transitions play a crucial role in determining the slow approach of the probability distribution $P(n, t)$ to its unique steady state $P_S(n)$. The equation for the steady-state distribution $P_S(n)$ can be written as [44]

$$0 = J(n+1) - J(n), \quad (2.6)$$

with $J(n)$ the probability current,

$$J(n) = T_-(n)P_S(n) - T_+(n-1)P_S(n-1). \quad (2.7)$$

Since $T_-(0)=0$ and $P_S(-1)=0$, it follows that $J(0)=0$ and $J(n)=0$ for all $n \geq 0$. Hence,

$$P_S(n) = \frac{T_+(n-1)}{T_-(n)} P_S(n-1) = P_S(0) \prod_{m=1}^n \frac{T_+(m-1)}{T_-(m)} \quad (2.8)$$

with $P_S(0) = 1 - \sum_{m=1}^{\infty} P_S(m)$. One finds that the stable and unstable fixed points of the deterministic rate equation are represented as minima and maxima, respectively, of the steady-state distribution $P_S(n)$ (see Fig. 2). The relative heights of the maxima depend on the system size N as illustrated in Fig. 3.

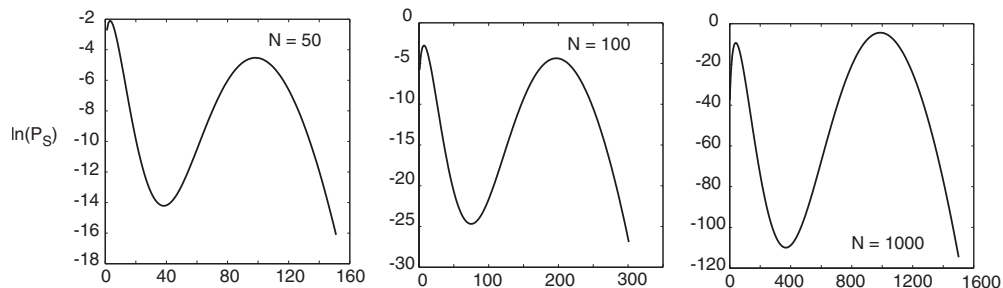


FIG. 3. Plots of steady-state distribution $P_S(n)$ for various system sizes N . Other parameters are $\gamma=4$, $\theta=0.87$, $f_0=2$

Note that approximating the neural master Eq. (2.3) by a neural Langevin equation would lead to exponentially large errors in the values of the peaks of the steady-state distribution, and consequently exponentially large errors in the calculation of the escape rates between metastable states (see Sec. III). The Langevin equation can be derived by carrying out a Kramers-Moyal expansion of the master equation [3,4]. First, introduce the rescaled variable $x=n/N$ and corresponding transition rates $N\Omega_{\pm}(x)=T_{\pm}(Nx)$, that is

$$\Omega_{+}(x)=f(x), \quad \Omega_{-}(x)=x. \quad (2.9)$$

Equation (2.3) can then be rewritten in the form

$$\begin{aligned} \frac{dP(x,t)}{dt} &= N[\Omega_{+}(x-1/N)P(x-1/N,t) + \Omega_{-}(x+1/N) \\ &\times P(x+1/N,t) - (\Omega_{+}(x) + \Omega_{-}(x))P(x,t)]. \end{aligned} \quad (2.10)$$

Treating x as a continuous variable and Taylor expanding terms on the right-hand side to second order in N^{-1} leads to the FP equation

$$\frac{\partial P(x,t)}{\partial t} = -\frac{\partial}{\partial x}[A(x)P(x,t)] + \frac{\epsilon^2}{2} \sum_{k=1}^M \frac{\partial^2}{\partial x^2}[B(x)P(x,t)] \quad (2.11)$$

with $\epsilon=N^{-1/2}$ and

$$A(x) = \Omega_{+}(x) - \Omega_{-}(x), \quad B(x) = \Omega_{+}(x) + \Omega_{-}(x). \quad (2.12)$$

The solution to the FP Eq. (2.11) determines the probability density function for a corresponding Ito stochastic process $X(t)$, which evolves according to a neural Langevin equation of the form

$$dX = A(X)dt + \epsilon b(X)dW(t), \quad (2.13)$$

with $b(x)^2=B(x)$. Here $W(t)$ denotes an independent Wiener process such that

$$\langle W(t) \rangle = 0, \quad \langle W(t)W(s) \rangle = \min(t,s). \quad (2.14)$$

The FP Eq. (2.11) has the steady-state solution

$$P_S(x) = \mathcal{A} \exp\left(2N \int^x \frac{\Omega_{+}(x') - \Omega_{-}(x')}{\Omega_{+}(x') + \Omega_{-}(x')} dx'\right), \quad (2.15)$$

where \mathcal{A} is a normalization factor. On the other hand, setting $n=Nx$ in Eq. (2.8), one finds that for large N (see also Sec. III),

$$P_S(x) = \mathcal{A}' \exp\left(N \int^x \ln \frac{\Omega_{+}(x')}{\Omega_{-}(x')} dx'\right) \quad (2.16)$$

with normalization factor \mathcal{A}' . Writing $P_S(x) \sim e^{-N\Phi(x)}$, we see that the stochastic potential $\Phi(x)$ associated with the FP equation differs from that of the underlying master equation, and this leads to exponentially large errors when calculating escape rates for example. Thus great care must be taken when approximating a neural (or chemical) master equation by a corresponding FP or Langevin equation [5–7].

III. ANALYSIS OF STOCHASTIC DYNAMICS IN THE BISTABLE REGIME

In order to explore the approach to steady state, let us rewrite the master equation (2.3) as the linear system

$$\frac{d\mathbf{p}}{dt} = \mathbf{Q}\mathbf{p}, \quad (3.1)$$

where $\mathbf{p}=[P(0,t), P(1,t), \dots]^T$ and \mathbf{Q} is the matrix

$$\mathbf{Q} = \begin{pmatrix} -T_{+}(0) & T_{-}(1) & 0 & \dots \\ T_{+}(0) & -T_{+}(1) - T_{-}(1) & T_{-}(2) & \dots \\ 0 & T_{+}(1) & -T_{+}(2) - T_{-}(2) & \dots \\ \vdots & \vdots & \vdots & \ddots \end{pmatrix}. \quad (3.2)$$

Suppose that we order the eigenvalues of \mathbf{Q} according to $\lambda_0 \geq \lambda_1 \geq \lambda_2 \geq \dots$. The Perron-Frobenius theorem implies that all the eigenvalues of \mathbf{Q} are real with the largest being a simple eigenvalue, $\lambda_0=0$, so that $\lambda_i < 0$ for $i \geq 1$. Suppose that the system is operating in a bistable regime so that there exist two stable fixed points x_{\pm} and one unstable fixed point x_0 of the corresponding deterministic rate Eq. (2.1). In the bistable regime, one finds that the second largest eigenvalue λ_1 differs from the other negative eigenvalues in the sense that it decays exponentially with the system size N , $|\lambda_1| \sim e^{-\tau_1 N}$ for $\tau_1 = \mathcal{O}(1)$, whereas $\lambda_i, i > 1$ are only weakly dependent on N . The existence of an exponentially small eigenvalue reflects the corresponding exponential dependence on N of the escape rates between the two stable fixed points of the deterministic system. Indeed, $\lambda_1 = -(r_{+} + r_{-})$ [5], where r_{-} is the escape rate from x_{-} to x_{+} and r_{+} is the escape rate from x_{+} to x_{-} . Expanding the solution to the master equation (2.3) in terms of the eigenvalues λ_i and corresponding eigenvectors $v_i(n)$,

$$P(n,t) = c_0 v_0(n) + c_1 v_1(n) e^{\lambda_1 t} + \dots \quad (3.3)$$

Since $\lambda_i < 0$ for all $i \geq 1$, it follows that $\lim_{t \rightarrow \infty} P(n,t) = c_0 v_0(n)$ and we can identify $v_0(n)$ with the steady-state distribution $P_S(n)$. The higher-order eigenmodes $v_i(n)$ for $i > 1$ will decay relatively rapidly, so that the approach to the steady-state will be dominated by the first eigenmode $v_1(n)$. In this section we show how the escape rates r_{\pm} and hence the eigenvalue λ_1 can be calculated by exploiting the fact that r_{\pm} are exponentially small functions of the system size N . Following previous studies of chemical master equations [5,35–39], we construct a quasistationary solution of the master equation using a WKB approximation. This leads to a corresponding Hamiltonian dynamical system that describes the most probable path of escape from a metastable state. The escape rates are then obtained by asymptotically matching the quasistationary solution with an appropriate inner solution in a neighborhood of the saddle point $x=x_0$. This is necessary in order to satisfy appropriate boundary conditions at x_0 . Finally, the long-term behavior of the bistable network can be represented in terms of a two-state Markov process describing transitions between the two metastable states $n_{\pm} = Nx_{\pm}$ [7].

A. WKB approximation

Let $\Pi(x)$ with $x=n/N$ denote a quasistationary solution associated with finding the network in the basin of attraction of one of the stable fixed points $x^*=x_{\pm}$:

$$0 = \Omega_+(x-1/N)\Pi(x-1/N) + \Omega_-(x+1/N)\Pi(x+1/N) - [\Omega_+(x) + \Omega_-(x)]\Pi(x). \quad (3.4)$$

Note that here x is treated as a continuous variable $x \in [0, \infty)$. We seek a WKB solution of the form

$$\Pi(x) \sim K(x)e^{-NS(x)}, \quad (3.5)$$

with $S(x^*)=0, K(x^*)=1$. Substituting Eq. (3.5) into Eq. (3.4), Taylor expanding with respect to N^{-1} , and collecting the $\mathcal{O}(1)$ terms gives

$$\sum_{r=\pm 1} \Omega_r(x)[e^{rS'(x)} - 1] = 0, \quad (3.6)$$

where $S' = dS/dx$. Mathematically speaking, Eq. (3.6) takes the form of a stationary Hamilton-Jacobi equation $H[x, S'(x)] = 0$ for S , with Hamiltonian

$$H(x, p) = \sum_{r=\pm 1} \Omega_r(x)[e^{rp} - 1] = x[e^{-p} - 1] + f(x)[e^p - 1]. \quad (3.7)$$

This suggests a corresponding classical mechanical interpretation, in which H determines the motion of a particle with position x and conjugate momentum p . A trajectory of the particle is given by the solution of Hamilton's equations

$$\dot{x} = \frac{\partial H}{\partial p} = \sum_{r=\pm 1} r\Omega_r(x)e^{rp} = -xe^{-p} + f(x)e^p \quad (3.8)$$

$$\dot{p} = -\frac{\partial H}{\partial x} = \sum_{r=\pm 1} \frac{\partial \Omega_r}{\partial x}(x)[e^{rp} - 1] = [e^{-p} - 1] + f'(x)[e^p - 1] \quad (3.9)$$

Here the time t should be viewed as a parameterization of paths rather than as a real time variable. Introducing the Lagrangian

$$L(x, \dot{x}) = p \cdot \dot{x} - H(x, p), \quad (3.10)$$

it follows that $S(x)$ with $S(x^*)=0$ corresponds to the classical action evaluated along the least-action trajectory from x^* to x ,

$$S(x) = \inf_{x(t_0)=x^*, x(T)=x} \int_0^T L(x, \dot{x}) dt. \quad (3.11)$$

In terms of the underlying stochastic process $X(t)$, the least-action path can be interpreted as the most probable fluctuational path from x^* to x (in the large N limit) [42,43]. Since $p=S'$ everywhere along this path, we have

$$S(x) = \int_{x^*}^x p(x') dx', \quad (3.12)$$

with the integral taken along the trajectory. It follows that the leading-order term in the WKB approximation is determined

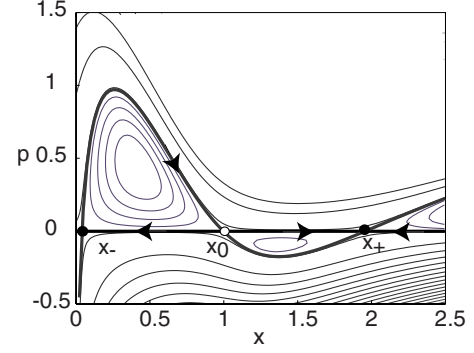


FIG. 4. (Color online) Phase portrait of Hamiltonian equations of motion for $\Omega_+(x)=f_0/(1+e^{-\gamma(x-\theta)})$ and $\Omega_-(x)=x$ with $\gamma=4$, $\theta=1.0$, and $f_0=2$. The zero energy solutions are shown as thicker curves.

by finding zero energy solutions $p=p(x)$ such that $H[x, p(x)]=0$. Given these zero energy solutions, the multiplicative factor $K(x)$ can be determined by solving the equation

$$H_p \frac{K'}{K} = -\frac{1}{2} p' H_{pp} - H_{px}, \quad (3.13)$$

with $H_p = \partial H[x, p(x)] / \partial p$ etc. Equation (3.13) is obtained by collecting the $\mathcal{O}(1/N)$ terms in the WKB solution of Eq. (3.4).

Since Eq. (3.6) is a quadratic in e^p , there are two classes of zero energy solution given by (see Fig. 4)

$$p = 0, \quad p = p_*(x) \equiv \ln \frac{\Omega_-(x)}{\Omega_+(x)}. \quad (3.14)$$

The classical equation of motion along the so-called *relaxation* trajectory $p=0$ is precisely the deterministic rate Eq. (2.1), which in the bistable regime has three fixed points x_{\pm}, x_0 . Motion along a neighborhood of a relaxation trajectory toward one of the two fixed points x_{\pm} characterizes the fast behavior of the system that is consistent with a Gaussian process in a neighborhood of the given fixed point. However, on exponentially long time scales we expect transitions between the two metastable states centered about x_{\pm} , and the most likely (optimal) path of escape will be along the so-called *activation* trajectory $p=p_*(x)$ from x_{\pm} to the saddle point x_0 . On crossing x_0 we expect the system to rapidly move along the relaxation trajectory to the other fixed point x_{\mp} . In Fig. 4 we illustrate the Hamiltonian phase space for a bistable neural network showing the constant energy solutions of the Hamiltonian given by Eq. (3.7); the zero energy activation and relaxation trajectories through the fixed points of the deterministic system are highlighted as thicker curves. After evaluating the factor $K(x)$ by solving Eq. (3.13), it follows that along an activation trajectory [39]

$$\Pi(x) = \frac{A}{\sqrt{\Omega_+(x)\Omega_-(x)}} e^{-NS(x)} \quad (3.15)$$

with

$$S(x) = \int^x \ln \frac{\Omega_-(y)}{\Omega_+(y)} dy, \quad (3.16)$$

whereas, along a relaxation trajectory $S=0$ and

$$\Pi(x) = \frac{B}{\Omega_+(x) - \Omega_-(x)} \quad (3.17)$$

for some constant B .

B. Calculation of escape rates

Given the WKB approximation, the rate of escape r_- from the metastable state centered about $x=x_-$ can be calculated by matching the quasistationary solutions with an appropriate inner solution in a neighborhood of the saddle point $x=x_0$ [5,35–39]. This is necessary since the quasistationary solutions (3.15) and (3.17) do not satisfy appropriate boundary conditions at the saddle point separating the two metastable states. We will briefly describe the method of Escudero and Kamenev [39], and then apply their result to the particular example of a bistable neural network. Escudero and Kamenev assume that there is a constant flux J through the saddle and then match the activation solution on one side of the saddle ($x < x_0$) with the relaxation solution on the other side of the saddle ($x > x_0$) using a diffusion approximation of the full master equation (2.3) in the vicinity of x_0 . The latter yields the FP [Eq. (2.11)], which can be rewritten in the form of a continuity relation

$$\frac{\partial}{\partial t} P(x,t) = - \frac{\partial}{\partial x} J(x,t) \quad (3.18)$$

with

$$J(x,t) = [\Omega_+(x) - \Omega_-(x)] P(x,t) - \frac{1}{2N} \frac{\partial}{\partial x} \{ [\Omega_+(x) + \Omega_-(x)] P(x,t) \}. \quad (3.19)$$

Substituting the quasistationary solution $\Pi(x,t) = \Pi(x)e^{-r_-t}$ into Eq. (3.18) and using the fact that r_- is exponentially small, gives

$$J = [\Omega_+(x) - \Omega_-(x)] \Pi(x) - \frac{1}{2N} \frac{\partial}{\partial x} \{ [\Omega_+(x) + \Omega_-(x)] \Pi(x) \}, \quad (3.20)$$

where J is the constant flux through the saddle. In a neighborhood of the saddle this equation can be Taylor expanded to leading order in $x-x_0$ and integrated to obtain the solution

$$\Pi(x) = \frac{JN}{\Omega_+(x_0)} e^{(x-x_0)^2/\sigma^2} \int_x^\infty e^{-(y-x_0)^2/\sigma^2} dy, \quad (3.21)$$

where

$$\sigma = \sqrt{\frac{2\Omega_+(x_0)}{N[\Omega'_+(x_0) - \Omega'_-(x_0)]}} \quad (3.22)$$

determines the size of the boundary layer around the saddle.

In order to match the activation and relaxation solutions, the following asymptotic behavior of the inner solution (3.21) is used,

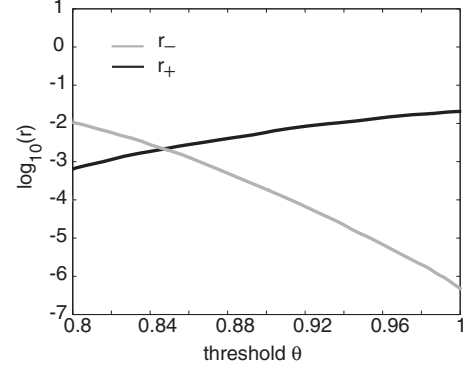


FIG. 5. Plot of calculated escape rates r_{\pm} for a bistable neural network as a function of the threshold θ . Other parameters are $\gamma = 4.0$, $f_0 = 2$, and $N = 20$. The escape rates are approximately equal for $\theta \approx 0.85$.

$$\Pi(x) = \begin{cases} \frac{NJ\sigma^2}{(x-x_0)\Omega_+(x_0)}, & x-x_0 \gg \sigma \\ \frac{NJ\sigma\sqrt{\pi}}{\Omega_+(x_0)} e^{(x-x_0)^2/\sigma^2}, & x_0-x \gg \sigma \end{cases}. \quad (3.23)$$

The solution to the right of the saddle matches the relaxation solution (3.17) since $\Omega_+(x) - \Omega_-(x) \approx (x-x_0)[\Omega'_+(x_0) - \Omega'_-(x_0)]$ for $x \approx x_0$ such that $B=J$. In order to match the solution on the left-hand side of the saddle with the activation solution (3.15), Taylor expand $S(x)$ about x_0 using $S'(x_0)=0$ and $S''(x_0)=-2/N\sigma^2$. It follows that

$$J = \frac{A\Omega_+(x_0)}{\sqrt{\Omega_+(x_0)\Omega_-(x_0)}} \sqrt{\frac{|S''(x_0)|}{2\pi N}} e^{-NS(x_0)}. \quad (3.24)$$

The final step in the analysis is to link the flux J with the escape rate r_- . This is achieved by integrating the continuity Eq. (3.18) over the interval $x \in [0, x_0]$ and using a reflecting boundary condition at $x=0$,

$$\frac{1}{r_-} = \frac{1}{J} \int_0^{x_0} \Pi(y) dy. \quad (3.25)$$

Since the activation solution is strongly peaked around the fixed point x_- , a Gaussian approximation of $\Pi(x)$ around x_- can be used to give the result [39]

$$r_- = \frac{\Omega_+(x_-)}{2\pi} \sqrt{|S''(x_0)| |S''(x_-)|} e^{-N[S(x_0) - S(x_-)]}. \quad (3.26)$$

Similarly, the escape rate from the metastable state x_+ is

$$r_+ = \frac{\Omega_+(x_+)}{2\pi} \sqrt{|S''(x_0)| |S''(x_+)|} e^{-N[S(x_0) - S(x_+)]}. \quad (3.27)$$

We now apply the above results to the particular case of a bistable neural network evolving according to a master equation with transition rates of Eq. (2.9). In particular, the variation of the calculated escape rates r_{\pm} with respect to the threshold θ is plotted in Fig. 5. As expected, r_+ (r_-) increases (decreases) as the threshold increases, reflecting the fact that the more active metastable state dominates at lower thresh-

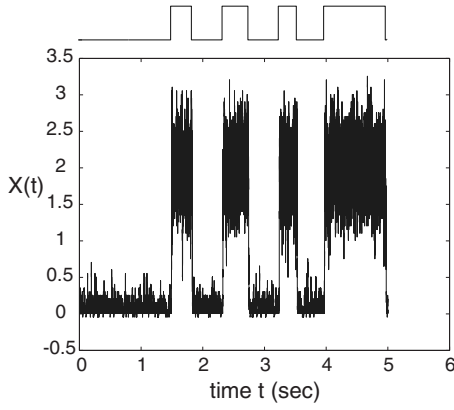


FIG. 6. Time series showing a single realization of the stochastic process $X(t)=N(t)/N$ where $N(t)$ is the birth-death process corresponding to the neural master equation (2.3). The parameters are $\theta=0.86$, $\gamma=4.0$, $f_0=2$, and $N=20$. The bistable nature of the process is clearly seen.

olds. It can also be seen that there is a narrow range of thresholds over which r_{\pm} are comparable; otherwise, one metastable state dominates. The bistable nature of the stochastic neural network is illustrated in Figs. 6 and 7 for different choices of threshold. It can be seen that the dynamics is characterized by sharp transitions between the two metastable states x_{\pm} combined with localized (Gaussianlike) fluctuations in a neighborhood of each state. Consistent with Fig. 5, lowering the threshold increases the relative time the network spends in the active state. (Note that the bistable nature of the system vanishes in the rescaled version of the master equation considered by Buice *et al.* [30,31], since it operates in a Poissonlike regime).

C. Bistable network as two-state Markov process

Having calculated the escape rates r_{\pm} , the long-term behavior of the stochastic bistable network can be approximated by a two-state Markov process that only keeps track of which metastable state the system is close to [7]

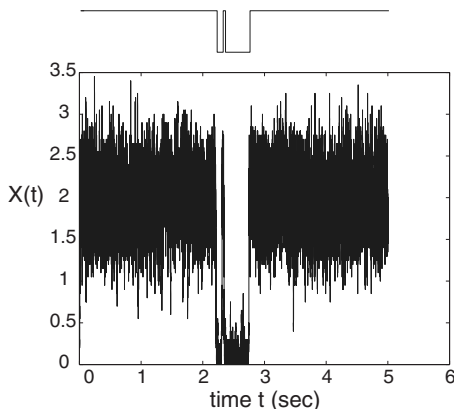


FIG. 7. Same as Fig. 6 except that $\theta=0.83$.

$$\frac{d}{dt} \begin{pmatrix} P_- \\ P_+ \end{pmatrix} = \hat{\mathbf{Q}} \begin{pmatrix} P_- \\ P_+ \end{pmatrix}, \quad \hat{\mathbf{Q}} = \begin{pmatrix} -r_- & r_+ \\ r_- & -r_+ \end{pmatrix}, \quad (3.28)$$

where P_{\pm} are the probabilities of being in a neighborhood of x_{\pm} . The matrix $\hat{\mathbf{Q}}$ has eigenvectors $\hat{\lambda}_0=0$ and $\hat{\lambda}_1=-(r_++r_-)$ and corresponding eigenvectors

$$\hat{\mathbf{v}}_0 = \begin{pmatrix} \frac{r_+}{r_++r_-} \\ \frac{r_-}{r_++r_-} \end{pmatrix}, \quad \hat{\mathbf{v}}_1 = \begin{pmatrix} \frac{1}{2} \\ -\frac{1}{2} \end{pmatrix}. \quad (3.29)$$

The eigenvalues of $\hat{\mathbf{Q}}$ are identical to the first two eigenvalues of the full matrix \mathbf{Q} of the master equation (3.1). Moreover, the two-component eigenvectors $\hat{\mathbf{v}}_j$ are reduced versions of the eigenvectors $v_j(n)$, $n \geq 0$ of \mathbf{Q} . That is

$$\hat{v}_{j,1} \approx \sum_{n=0}^{n_0} v_j(n), \quad \hat{v}_{j,2} \approx \sum_{n=n_0}^{\infty} v_j(n), \quad j=0,1. \quad (3.30)$$

In particular, $\hat{\mathbf{v}}_0$ determines the steady-state probability of being in the neighborhood of either metastable state. Note that the two-state model generates an exponential density for the residence times within a given metastable state. This captures the behavior of the full master equation at large residence times but fails to capture the short-term dynamics associated with relaxation trajectories within a neighborhood of the metastable state.

IV. MULTIPLE POPULATION MODEL

Now suppose that there exist M homogeneous neuronal populations labeled $i=1, \dots, M$, each of size N . Assume that all neurons of a given population are equivalent in the sense that the effective pairwise synaptic interaction between a neuron of population i and a neuron of population j only depends on i and j . Suppose that there are $N_k(t)$ active neurons in the k th population. The state or configuration of the network is now specified by the vector $\mathbf{N}(t)=[N_1(t), N_2(t), \dots, N_M(t)]$, where each $N_i(t)$ is treated as a stochastic variable that evolves according to a one-step jump Markov process. Let $P(\mathbf{n}, t)=\text{Prob}[\mathbf{N}(t)=\mathbf{n}]$ denote the probability that the network of interacting populations has configuration $\mathbf{n}=(n_1, n_2, \dots, n_M)$ at time t , $t>0$, given some initial distribution $P(\mathbf{n}, 0)$. The probability distribution is then taken to evolve according to a master equation of the form [29–31]

$$\frac{dP(\mathbf{n}, t)}{dt} = \sum_{k=1}^M \sum_{r=\pm 1} [T_{k,r}(\mathbf{n} - r\mathbf{e}_k)P(\mathbf{n} - r\mathbf{e}_k, t) - T_{k,r}(\mathbf{n})P(\mathbf{n}, t)]. \quad (4.1)$$

Here \mathbf{e}_k denotes the unit vector whose k th component is equal to unity. The corresponding transition rates are given by

$$T_{k,-1}(\mathbf{n}) = \alpha_k n_k, \quad T_{k,+1}(\mathbf{n}) = N f \left(\sum_l w_{kl} n_l / N + h_k \right), \quad (4.2)$$

where α_k are rate constants, w_{kl} is the effective synaptic weight from the l th to the k th population, and h_k are external

inputs. Equation (4.1) is supplemented by the boundary conditions $P(\mathbf{n}, t) \equiv 0$ if $n_i = -1$ for some i . The master equation preserves the normalization condition $\sum_{n_1 \geq 0} \sum_{n_M \geq 0} P(\mathbf{n}, t) = 1$ for all $t \geq 0$.

Introduce the rescaled variables $x_k = n_k/N$ and corresponding transition rates

$$\Omega_{k,-1}(\mathbf{x}) = \alpha_k x_k, \quad \Omega_{k,1}(\mathbf{x}) = f\left(\sum_l w_{kl} x_l + h_k\right). \quad (4.3)$$

Carrying out a Kramers-Moyal expansion to second order then leads to the multivariate FP equation

$$\frac{\partial P(\mathbf{x}, t)}{\partial t} = - \sum_{k=1}^M \frac{\partial}{\partial x_k} [A_k(\mathbf{x}) P(\mathbf{x}, t)] + \frac{\epsilon^2}{2} \sum_{k=1}^M \frac{\partial^2}{\partial x_k^2} [B_k(\mathbf{x}) P(\mathbf{x}, t)] \quad (4.4)$$

with $\epsilon = N^{-1/2}$,

$$A_k(\mathbf{x}) = \Omega_{k,1}(\mathbf{x}) - \Omega_{k,-1}(\mathbf{x}) \quad (4.5)$$

and

$$B_k(\mathbf{x}) = \Omega_{k,1}(\mathbf{x}) + \Omega_{k,-1}(\mathbf{x}). \quad (4.6)$$

The solution to the FP Eq. (4.4) determines the probability density function for a corresponding stochastic process $\mathbf{X}(t) = [X_1(t), \dots, X_M(t)]$, which evolves according to a neural Langevin equation of the form

$$dX_k = A_k(\mathbf{X}) dt + \epsilon b_k(\mathbf{X}) dW_k(t). \quad (4.7)$$

with $b_k(\mathbf{x})^2 = B_k(\mathbf{x})$. Here $W_k(t)$ denotes an independent Wiener process such that

$$\langle W_k(t) \rangle = 0, \quad \langle W_k(t) W_l(s) \rangle = \delta_{k,l} \min(t, s). \quad (4.8)$$

As in the one-population model, the FP or Langevin equation captures the relatively fast stochastic dynamics within the basin of attraction of a stable fixed point (or limit cycle) of the corresponding deterministic rate equations

$$\frac{du_k}{dt} = -\alpha_k u_k + f\left(\sum_l w_{kl} u_l + h_k\right). \quad (4.9)$$

However, in order to analyze state transitions between basins of attraction, it is necessary to consider a higher-dimensional version of the asymptotic methods presented in Sec. III. In this section we first show how the neural Langevin equation can be used to analyze noise-induced oscillations in a two-population network. We then describe how the WKB approximation and associated Hamiltonian formulation can be extended to multiple populations.

A. Noise-induced amplification of oscillations in E-I network

One of the major differences between the single and multipopulation models is that the latter can support limit cycle oscillations. The simplest and best studied example is a two-population model consisting of an excitatory population interacting with an inhibitory population as shown in Fig. 8. The associated mean-field Eq. (4.9) for this E-I (excitatory-inhibitory) network reduces to the pair of equations

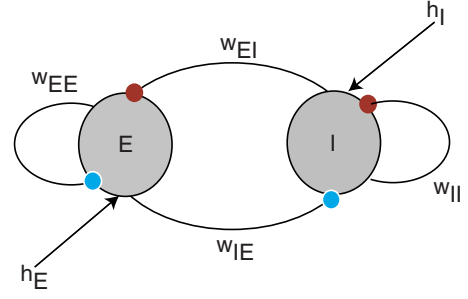


FIG. 8. (Color online) Two-population E-I network

$$\frac{du_E}{dt} = -u_E + f(w_{EE}u_E - w_{EI}u_I + h_E),$$

$$\frac{du_I}{dt} = -u_I + f(w_{IE}u_E - w_{II}u_I + h_I), \quad (4.10)$$

where we have set $\alpha_{E,I} = 1$ for simplicity and we have made the sign of the weights explicit by taking $w_{kl} \geq 0$ for all $k, l = E, I$. The bifurcation structure of the two-population Wilson-Cowan model given by Eqs. (4.10) has been analyzed in detail elsewhere [50]. An equilibrium (u_E^*, u_I^*) is obtained as a solution of the pair of equations

$$u_E^* = f(w_{EE}u_E^* - w_{EI}u_I^* + h_E),$$

$$u_I^* = f(w_{IE}u_E^* - w_{II}u_I^* + h_I). \quad (4.11)$$

These can be inverted to yield

$$h_E = f^{-1}(u_E^*) - w_{EE}u_E^* + w_{EI}u_I^*,$$

$$h_I = f^{-1}(u_I^*) - w_{IE}u_E^* + w_{II}u_I^*. \quad (4.12)$$

As a simplification, let us take the gain function f to be the simple sigmoid $f(u) = (1 + e^{-u})^{-1}$. Using the fact that the sigmoid function then satisfies $f' = f(1-f)$ and applying the fixed-point equations allows us to represent the associated Jacobian in the form

$$\mathbf{J} = \begin{pmatrix} -1 + w_{EE}u_E^*(1-u_E^*) & -w_{EI}u_E^*(1-u_E^*) \\ w_{IE}u_I^*(1-u_I^*) & -1 - w_{II}u_I^*(1-u_I^*) \end{pmatrix}.$$

An equilibrium will be stable provided that the eigenvalues λ_{\pm} of \mathbf{J} have negative real parts, where

$$\lambda_{\pm} = \frac{1}{2} (\text{Tr } \mathbf{J} \pm \sqrt{[\text{Tr } \mathbf{J}]^2 - 4 \text{Det } \mathbf{J}}). \quad (4.13)$$

This leads to the stability conditions $\text{Tr } \mathbf{J} < 0$ and $\text{Det } \mathbf{J} > 0$. In order to construct a phase diagram in the (h_E, h_I) -plane for a fixed weight matrix \mathbf{w} , we express u_I^* as a function of u_E^* by imposing a constraint on the eigenvalues λ_{\pm} and then substitute the resulting function into Eqs. (4.12). This yields bifurcation curves in the (h_E, h_I) -plane that are parametrized by u_E^* and $0 < u_E^* < 1$ (see Fig. 9). For example, the constraint

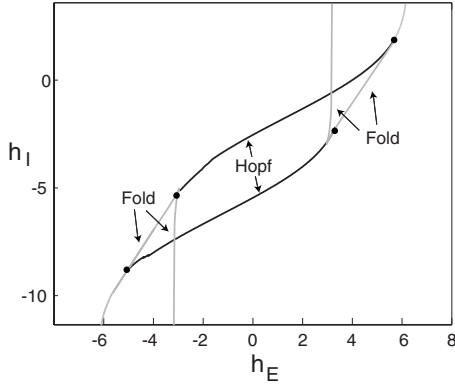


FIG. 9. Phase diagram of two-population Wilson-Cowan model (4.10) for fixed set of weights $w_{EE}=w_{IE}=w_{EI}=10$, $w_{II}=4$. The dots correspond to Takens-Bogdanov bifurcation points

$$\text{Tr } \mathbf{J} \equiv -2 + w_{EE}u_E^*(1 - u_E^*) - w_{II}u_I^*(1 - u_I^*) = 0 \quad (4.14)$$

with $\text{Det } \mathbf{J} > 0$ determines Hopf bifurcation curves where a pair of complex-conjugate eigenvalues cross the imaginary axis. Since the trace is a quadratic function of u_E^*, u_I^* , we obtain two Hopf branches. Similarly, the constraint $\text{Det } \mathbf{J} = 0$ with $\text{Tr } \mathbf{J} < 0$ determines saddle-node or fold bifurcation curves where a single real eigenvalue crosses zero. The saddle-node curves have to be determined numerically, since the determinant is a quartic function of u_E^*, u_I^* .

Consider a point in parameter space where there exists a single fixed point of the mean-field Eqs. (4.10). Suppose that the fixed point is a stable focus so that its Jacobian has a pair of complex-conjugate eigenvalues. The corresponding deterministic network exhibits transient or subthreshold oscillations that decay at a rate given by the real part of the eigenvalues. We will show how intrinsic noise can convert these transient oscillations into large amplitude sustained coherent oscillations, giving rise to a peak in the corresponding power spectrum (quasicycles). We proceed along similar lines to recent work on biochemical oscillations in cellular systems [40,41]. The first step is to decompose the solution to the neural Langevin Eq. (4.7) as

$$X_k = u_k^* + \epsilon \eta_k(t) \quad (4.15)$$

such that $A_k(\mathbf{u}^*) = 0$, where $\mathbf{u} = (u_E, u_I)$. Taylor expanding Eq. (4.7) to the first order in ϵ then implies that η_k satisfies the linear Langevin equation

$$d\eta_k = \sum_{l=E,I} J_{kl} \eta_l dt + b_k(\mathbf{u}^*) dW_k(t), \quad (4.16)$$

where $J_{kl} = \partial A_k / \partial x_l |_{\mathbf{x}=\mathbf{u}^*}$. Introducing the white-noise processes $\xi_k(t)$ according to $dW_k(t) = \xi_k(t) dt$ with

$$\langle \xi_k(t) \rangle = 0, \quad \langle \xi_k(t) \xi_l(t') \rangle = \delta_{k,l} \delta(t - t'), \quad (4.17)$$

we can rewrite the Langevin equation in the form

$$\frac{d\eta_k}{dt} = \sum_{l=E,I} J_{kl} \eta_l + b_k(\mathbf{u}^*) \xi_k(t). \quad (4.18)$$

Let $\tilde{\eta}_k(\omega)$ denote the Fourier transform of $\eta_k(t)$ with

$$\tilde{\eta}_k(\omega) = \int_{-\infty}^{\infty} e^{-i\omega t} \eta_k(t) dt.$$

Taking Fourier transforms of Eq. (4.18) gives

$$-i\omega \tilde{\eta}_k(\omega) = \sum_{l=E,I} J_{kl} \tilde{\eta}_l(\omega) + b_k(\mathbf{u}^*) \tilde{\xi}_k(\omega). \quad (4.19)$$

This can be rearranged to give

$$\tilde{\eta}_k(\omega) = \sum_{l=E,I} \Phi_{kl}^{-1}(\omega) b_l(\mathbf{u}^*) \tilde{\xi}_l(\omega) \quad (4.20)$$

with $\Phi_{kl}(\omega) = -i\omega \delta_{k,l} - J_{kl}$. The Fourier transform of the white-noise process $\xi_k(t)$ has the correlation function

$$\langle \tilde{\xi}_k(\omega) \tilde{\xi}_l(\omega') \rangle = 2\pi \delta_{k,l} \delta(\omega + \omega'). \quad (4.21)$$

The power spectrum is defined according to

$$2\pi \delta(0) P_k(\omega) = \langle |\tilde{\eta}_k(\omega)|^2 \rangle, \quad (4.22)$$

so that Eqs. (4.20) and (4.21) give

$$P_k(\omega) = \sum_{l=E,I} |\Phi_{kl}^{-1}(\omega)|^2 B_l(\mathbf{u}^*), \quad (4.23)$$

with $B_l(\mathbf{u}^*) = b_l(\mathbf{u}^*)^2$. The right-hand side can be evaluated explicitly to yield

$$P_k(\omega) = \frac{\beta_k + \gamma_k \omega^2}{|D(\omega)|^2} \quad (4.24)$$

with $D(\omega) = \text{Det } \Phi(\omega) = -\omega^2 + i\omega \text{Tr } \mathbf{J} + \text{Det } \mathbf{J}$ and

$$\beta_E = J_{22}^2 B_E(\mathbf{u}^*) + J_{12}^2 B_I(\mathbf{u}^*), \quad \gamma_E = B_E(\mathbf{u}^*) \quad (4.25)$$

$$\beta_I = J_{21}^2 B_E(\mathbf{u}^*) + J_{11}^2 B_I(\mathbf{u}^*), \quad \gamma_I = B_I(\mathbf{u}^*). \quad (4.26)$$

Finally, evaluating the denominator and using the stability conditions $\text{Tr } \mathbf{J} < 0$, $\text{Det } \mathbf{J} > 0$, we have [40]

$$P_k(\omega) = \frac{\beta_k + \gamma_k \omega^2}{(\omega^2 - \Omega_0^2)^2 + \Gamma^2 \omega^2}, \quad (4.27)$$

where we have set $\Gamma = \text{Tr } \mathbf{J}$ and $\Omega_0^2 = \text{Det } \mathbf{J}$.

In Fig. 10, we compare our analytical calculation of the spectrum for subthreshold oscillations in an E-I pair with direct simulations of the full master equation (2.3). We choose a point in parameter space that lies just above the upper Hopf curve in Fig. 9 by taking $h_E = 0, h_I = -2$. The only fixed point is a stable focus. It can be seen in Fig. 10(a) that the spectrum exhibits a strong peak at a frequency $\omega \approx 2$, which is close to the Hopf frequency of limit cycle oscillations generated by crossing the nearby Hopf bifurcation boundary by decreasing the inhibitory input h_I . Sample trajectories for u_E and u_I also indicate oscillatorylike behavior [see Fig. 9(b)].

Note that it is also possible to extend the above spectral analysis to the case where the mean-field equations support a limit cycle oscillation by using Floquet theory [41]. However, a more relevant approach within the neural context would be to carry out a phase reduction of the underlying Langevin equation after converting it from the Ito to Stratonovich interpretation (so the standard rules of calculus can

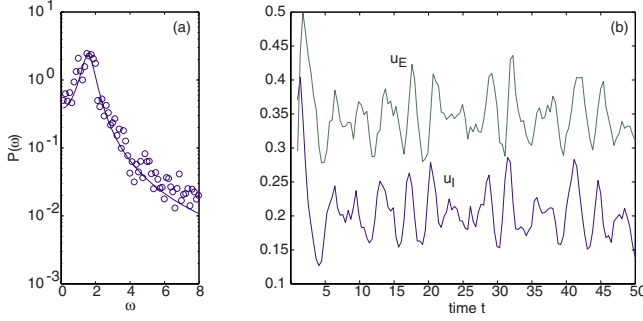


FIG. 10. (Color online) Noise-amplification of subthreshold oscillations in an E-I network. (a) Power spectrum of fluctuations (solid curve) obtained by Fourier transforming the Langevin Eq. (4.18). Data points are from stochastic simulations of full master equation with $N=1000$, averaged over 100 samples. (b) Sample trajectories obtained from stochastic simulations of full master equation with $N=100$. Same weight parameter values as Fig. 9 with $h_E=0$ and $h_I=-2$.

be applied [45]). This would then provide a framework for studying the effects of intrinsic noise on the synchronization of synaptically coupled E-I networks, each of which exhibits limit cycle oscillations in the mean-field limit. One application of such a model is to stimulus-induced oscillations and synchrony in primary visual cortex model, where each E-I network is interpreted as a cortical column consisting of reciprocally coupled populations of excitatory and inhibitory neurons [46,47].

B. Metastable states and WKB approximation for multiple populations

It is clear from Fig. 9 that there also exist parameter regimes in which the deterministic E-I network exhibits bistability due to the emergence of an additional stable fixed point via a fold or saddle-node bifurcation. Unfortunately, the analysis of metastability in a stochastic multipopulation model is considerably more involved than the one-population case. Here we briefly describe how to generalize the WKB method of Sec. III (see Refs. [35,42,43] for more details). Let $\Pi(\mathbf{x})$ and $\mathbf{x}=\mathbf{n}/N$ denote the quasistationary probability distribution associated with finding the network in the neighborhood of a stable fixed point S of the mean-field Eqs. (4.9). That is

$$\sum_{k=1}^M \sum_{r=\pm 1} [\Omega_{k,r}(\mathbf{x} - r\mathbf{e}_k/N) \Pi(\mathbf{x} - r\mathbf{e}_k/N) - \Omega_{k,r}(\mathbf{x}) \Pi(\mathbf{x})] = 0. \quad (4.28)$$

Following the analysis of the one-population model, we seek a solution that has the WKB form

$$\Pi(\mathbf{x}) \sim K(\mathbf{x}) e^{-NW(\mathbf{x})}, \quad K(S) = 1, W(S) = 0. \quad (4.29)$$

Substituting into the stationary master equation (4.28) and collecting $\mathcal{O}(1)$ terms gives the Hamilton-Jacobi equation

$$H(\mathbf{x}, \mathbf{p}) \equiv \sum_{r=\pm 1} \sum_{k=1}^M \Omega_{k,r}(\mathbf{x}) [e^{rp_k} - 1] = 0, \quad (4.30)$$

where $p_k = \partial W / \partial x_k$. Similarly, collecting $\mathcal{O}(1/N)$ terms generates a differential equation for the factor K ,

$$\sum_i \frac{\partial H}{\partial p_i} \frac{\partial K}{\partial x_i} = - \left[\sum_i \frac{\partial^2 H}{\partial p_i \partial x_i} + \frac{1}{2} \sum_{i,j} \frac{\partial^2 W}{\partial x_i \partial x_j} \frac{\partial^2 H}{\partial p_i \partial p_j} \right] K. \quad (4.31)$$

Under the corresponding classical mechanical interpretation, the associated Hamiltonian H determines the motion of a particle with position vector $\mathbf{x} \in \mathbb{R}^M$ and conjugate momentum vector \mathbf{p} . A trajectory of the particle parametrized by t is given by the solution of Hamilton's equations

$$\dot{x}_k = \frac{\partial H}{\partial p_k} = \sum_{r=\pm 1} r \Omega_{k,r}(\mathbf{x}) e^{rp_k}, \quad (4.32)$$

$$\dot{p}_k = - \frac{\partial H}{\partial x_k} = \sum_{r=\pm 1} \sum_{l=1}^M \frac{\partial \Omega_{l,r}}{\partial x_k}(\mathbf{x}) [e^{rp_l} - 1] \quad (4.33)$$

given the initial conditions $[\mathbf{x}(t_0), \mathbf{p}(t_0)]$ in phase space. Introducing the Lagrangian

$$L(\mathbf{x}, \dot{\mathbf{x}}) = \mathbf{p} \cdot \dot{\mathbf{x}} - H(\mathbf{x}, \mathbf{p}), \quad (4.34)$$

it follows that $W(\mathbf{x})$ with $W(S)=0$ corresponds to the classical action evaluated along the least-action trajectory from S to \mathbf{x} [42],

$$W(\mathbf{x}) = \inf_{\mathbf{x}(t_0)=S, \mathbf{x}(T)=\mathbf{x}} \int_0^T L(\mathbf{x}, \dot{\mathbf{x}}) dt. \quad (4.35)$$

Since $p_k = \partial_k W$ everywhere along this path, it follows that

$$W(\mathbf{x}) = \int_S^{\mathbf{x}} p(\mathbf{x}') \cdot d\mathbf{x}', \quad (4.36)$$

with the line integral taken along the trajectory. Since S is a fixed point of the mean-field Eq. (4.9), that is, $\sum_{r=\pm 1} r \Omega_{k,r}(S) = 0$ for all $k=1, \dots, M$, it can also be shown that $(S, 0)$ is a hyperbolic fixed point of the Hamiltonian dynamical system given by Eqs. (4.32) and (4.33). It follows that along any most probable functional path starting from S we have $\lim_{t \rightarrow \infty} [\mathbf{x}(t), \mathbf{p}(t)] = (S, 0)$ so that one should take $t_0 = -\infty$ in Eq. (4.35). From a dynamical systems perspective, the most probable paths form the unstable manifold of the fixed point $(S, 0)$. The stable manifold is given by $\mathbf{p}=0$ and consists of trajectories given by solutions of the mean-field Eq. (4.9).

In contrast to the one-population model, it is no longer possible to obtain analytical expressions for the quasistationary density. However, one can numerically evaluate $W(\mathbf{x})$ and $K(\mathbf{x})$ by evolving Hamilton's equations from initial points $[\mathbf{x}, \mathbf{p}(\mathbf{x})]$ in a neighborhood of $(S, 0)$ with $\mathbf{p}(\mathbf{x})$ determined using a Gaussian approximation of W . Let $Z_{ij} = \partial_i \partial_j W(\mathbf{x})$ denote the Hessian matrix of $W(\mathbf{x})$ [38]. A dy-

namical equation for \mathbf{Z} can be derived by differentiating equation $H[\mathbf{x}, \mathbf{p}(\mathbf{x})]=0$ twice with respect to \mathbf{x} using Hamilton's equations and

$$\frac{d}{dx_k} = \frac{\partial}{\partial x_k} + \sum_l \frac{dp_l}{dx_k} \frac{\partial}{\partial p_l}.$$

This yields the matrix equation

$$\begin{aligned} \dot{Z}_{ij} &\equiv \sum_k \frac{\partial H}{\partial p_k} \frac{\partial Z_{ij}}{\partial x_k} \\ &= - \left[\sum_{k,l} \frac{\partial^2 H}{\partial p_k \partial p_l} Z_{ik} Z_{jl} + \sum_l \frac{\partial^2 H}{\partial x_i \partial p_l} Z_{jl} \right. \\ &\quad \left. + \sum_l \frac{\partial^2 H}{\partial x_j \partial p_l} Z_{il} + \frac{\partial^2 H}{\partial x_i \partial x_j} \right]. \end{aligned} \quad (4.37)$$

At the fixed point $(S, 0)$ we have $\dot{\mathbf{Z}}=0$ and

$$\begin{aligned} \frac{\partial^2 H}{\partial x_l \partial p_k} &= \sum_{r=\pm 1} r \frac{\partial \Omega_{k,r}}{\partial x_l}(S) \equiv A_{kl}, \\ \frac{\partial^2 H}{\partial p_k \partial p_l} &= \delta_{k,l} \sum_{r=\pm 1} \Omega_{k,r}(S) \equiv B_{kl}, \\ \frac{\partial^2 H}{\partial x_k \partial x_l} &= 0 \end{aligned} \quad (4.38)$$

so that the Hessian evaluated at S is given by the solution to the algebraic Riccati equation

$$\mathbf{Z}(S)\mathbf{B}\mathbf{Z}(S) + \mathbf{Z}(S)\mathbf{A} + \mathbf{A}'\mathbf{Z}(S) = 0. \quad (4.39)$$

It can be shown that if $\text{Tr } \mathbf{A} \neq 0$ then there are exactly four solutions for $\mathbf{Z}(S)$: one of full rank, two of unit rank, and the trivial solution $\mathbf{Z}(S)=0$ [43]. Since the point S is a local minimum of $W(\mathbf{x})$, it follows that only the full rank solution is physically relevant and that in a small neighborhood of S we have the Gaussian approximation

$$W(\mathbf{x}) \approx -\frac{1}{2} \sum_{i,j} Z_{ij}(S) [x_i - x_i(S)] [x_j - x_j(S)] \quad (4.40)$$

with $\mathbf{Z}(S)$ the unique solution to the Riccati equation. It follows that $p_i(\mathbf{x}) \approx \sum_j Z_{ij}(S) [x_j - x_j(S)]$ and

$$\Pi(\mathbf{x}) \sim \exp \left\{ -\frac{N}{2} \sum_{i,j} Z_{ij}(S) [x_i - x_i(S)] [x_j - x_j(S)] \right\}. \quad (4.41)$$

The latter is also the solution to the corresponding FP Eq. (4.4), linearized about the fixed point S [3].

Having obtained the WKB approximation that matches the Gaussian approximation around, it remains to match with an inner solution close to the boundary $\partial\mathcal{M}$ of the basin of attraction. This is necessary, since the WKB solution does not satisfy the appropriate boundary condition on $\partial\mathcal{M}$. Typically, one either takes an absorbing boundary condition $P_0(\mathbf{x})=0$ on $\partial\mathcal{M}$ or one assumes that there is a constant flux $J(\mathbf{x})$ through the boundary that is determined self-

consistently. Following standard problems in classical transition rate theory, suppose that the deterministic network described by the mean-field Eq. (4.9) is bistable so that there exist two stable fixed points S, S' separated by a saddle point Q that lies on the separatrix $\partial\mathcal{M}$. In this case the most probable path from S to S' is through Q and the behavior around Q dominates the matched asymptotics. Provided that certain additional constraints hold, it can be shown that the transition rate takes the form [43]

$$\lambda_0 = \frac{\lambda_+(Q)}{2\pi} \left[\frac{\det \mathbf{Z}(S)}{\det \mathbf{Z}(Q)} \right]^{1/2} K(Q) e^{-W(Q)/N}, \quad (4.42)$$

where $\lambda_+(Q)$ is the positive eigenvalue of the Jacobian obtained by the linearizing the mean-field equation about Q . In general, the geometry of the trajectories in phase space makes the calculation of transition rates in the multidimensional case computationally challenging. However, an efficient numerical method called ‘‘transition path sampling’’ has recently been developed that allows one to study transition pathways for rare events in complex systems which can then be used to extract important physical quantities such as transition rates from metastable states [51].

C. Continuum neural field model

One of the distinct features of neural systems compared to chemical systems is that when spatial degrees of freedom are taken into account, the former involves nonlocal interactions rather than diffusive interactions. That is, it is common to model large-scale cortical networks in terms of spatially distributed populations labeled by spatial coordinates $\mathbf{q} \in \mathbb{R}^2$. In the deterministic limit, these continuum networks evolve according to neural field equations of the form [34]

$$\begin{aligned} \frac{\partial u_k(\mathbf{q}, t)}{\partial t} &= -\alpha_k u_k(\mathbf{q}, t) \\ &\quad + f \left[\sum_{l=E,I} \int w_{kl}(\mathbf{q}, \mathbf{q}') u_l(\mathbf{q}', t) d\mathbf{q}' + h_k(\mathbf{q}, t) \right], \end{aligned} \quad (4.43)$$

where $k, l=E, I$ specifies whether a given population is excitatory or inhibitory. The synaptic weight distributions $w_{kl}(\mathbf{q}, \mathbf{q}')$ specify the form of the nonlocal interactions. The associated stochastic neural field model is described in terms of a probability functional satisfying an infinite-dimensional version of the master equation (4.1). Under the diffusion approximation, this reduces to a functional FP equation of the form

$$\begin{aligned} \frac{\delta P([\mathbf{x}], t)}{\delta t} &= - \sum_{k=E,I} \int \frac{\delta}{\delta x_k(\mathbf{q})} [A_{k,\mathbf{q}}([\mathbf{x}]) P([\mathbf{x}], t)] \\ &\quad + \frac{\epsilon^2}{2} \sum_{k=E,I} \frac{\delta^2}{\delta x_k(\mathbf{q})^2} [B_{k,\mathbf{q}}([\mathbf{x}]) P([\mathbf{x}], t)], \end{aligned} \quad (4.44)$$

with $[\mathbf{x}] = \{(x_E(\mathbf{q}), x_I(\mathbf{q}))\}, \mathbf{q} \in \mathbb{R}^2$,

$$A_{k,\mathbf{q}}([\mathbf{x}]) = -\alpha_k x_k(\mathbf{q}) + f_{k,\mathbf{q}}([\mathbf{x}]),$$

$$B_{k,q}([\mathbf{x}]) = \alpha_k x_k(\mathbf{q}) + f_{k,q}([\mathbf{x}]),$$

and

$$f_{k,q}([\mathbf{x}]) = f \left[\sum_{l=E,I} \int w_{kl}(\mathbf{q}, \mathbf{q}') x_l(\mathbf{q}', t) d\mathbf{q}' + h_k(\mathbf{q}, t) \right].$$

It has previously been shown that deterministic neural field models support a variety of spatially coherent states including spatially periodic patterns arising via Turinglike instabilities [34,52–55]. In the case of homogeneous weight distributions, one could apply Fourier methods to the FP Eq. (4.44) in order to analyze the effects of intrinsic noise on such pattern forming instabilities [48]. One could also extend the analysis of quasicycles to the spatial domain, following along similar lines to a recent study of a diffusive predator-prey model [56]. However, as in the case of finite population models, the FP Eq. (4.44) would not take proper account of noise-induced transitions to other metastable states.

V. DISCUSSION

In this paper we have shown how techniques from the study of chemical master equations can be carried over to that of a scaled version of the neural master equation introduced by Buice *et al.* [30,31]. The latter can be viewed as a stochastic version of the Wilson-Cowan model of neural population dynamics in which noise is treated intrinsically. We focused on two particular effects of intrinsic noise fluctuations. First, we calculated exponentially small escape rates between metastable states of a one-population model using a WKB approximation and matched asymptotics; corrections to mean-field equations based on a system-size expansion (or loop expansion in the corresponding path-integral formulation) are no longer appropriate. Second, we analyzed quasicycles in an E-I network by determining the power spectrum of the associated neural Langevin equation.

A major outstanding question is to what extent the master-equation formulation captures the types of statistical fluctuations in population activity that can be observed in real nervous tissue. Buice and Cowan [30] have used path-integral methods and renormalization-group theory to establish that a continuum version of the stochastic Wilson-Cowan model belongs to the universality class of directed percolation, and consequently exhibits power-law behavior suggestive of many measurements of spontaneous cortical activity *in vitro* and *in vivo* [57,58]. However, the existence of power-law behavior is controversial [59]. Moreover, it is likely that a variety of different stochastic models could exhibit behavior consistent with what is observed experimentally. Therefore, can one use multiscale analysis to derive a master equation of population dynamics (or perhaps a different type of stochastic Wilson-Cowan model) starting from more detailed microscopic models? That is, the master-equation formulation of stochastic neurodynamics developed here and elsewhere [29–31] is a phenomenological representation of sto-

chasticity at the population level. It is not derived from a detailed microscopic model of synaptically coupled spiking neurons, and it is not yet clear under what circumstances such a microscopic model would yield population activity consistent with the master-equation approach. Nevertheless, if one views the Wilson-Cowan rate equations [33,34] as an appropriate description of large-scale neural activity in the deterministic limit, it is reasonable to explore ways of adding noise to such equations from a top-down perspective. One possibility is to consider a Langevin version of the Wilson-Cowan equations involving some form of extrinsic spatiotemporal white noise [48,49], whereas another is to view the Wilson-Cowan rate equations as the thermodynamic limit of an underlying master equation that describes the effects of intrinsic noise [29–32]. As we have highlighted in this paper, the two formulations are not equivalent.

One possible application of the master-equation formulation of neural population dynamics is modeling noise-induced switching during binocular rivalry. Binocular rivalry concerns the phenomenon whereby perception switches back and forth between different images presented to either eye [60,61]. Recordings from the brain and reports by human subjects during binocular rivalry tasks show eye dominance time statistics that may be fit to a gamma distribution [62]. In addition, statistical analysis of such data shows little correlation between one dominance time and the next [62–64]. This suggests that the switching between one eye's dominance and the next may be largely driven by a stochastic process. One possibility is that the inputs arriving at the network encoding rivalry are stochastic, so that the noise is extrinsic. A number of recent models have examined dominance switching times due to additive noise terms in a competitive Wilson-Cowan model with additional slow adapting variables [65–67]. On the other hand, Laing and Chow [68] considered a deterministic spiking neuron model of binocular rivalry in which the statistics of the resulting dominance times appeared noisy due to the aperiodicity of the high-dimensional system's trajectories. The latter is suggestive of an effective intrinsic noise source within a rate-based population model. One important issue is whether the switching time statistics is better captured by noise-induced transitions in a bistable network or noise-induced amplification of sub-threshold oscillations (quasicycles). In order to study this within the master equation framework, it will be necessary to incorporate some form of slow adaptation into the stochastic Wilson-Cowan model.

ACKNOWLEDGMENTS

This publication was based on work supported in part by the National Science Foundation Grant No. DMS-0813677 and by Award No. KUK-C1-013-4 by King Abdullah University of Science and Technology (KAUST). P.C.B. was also partially supported by the Royal Society Wolfson Foundation.

- [1] P. S. Swain, M. B. Elowitz, and E. D. Siggia, *Proc. Natl. Acad. Sci. U.S.A.* **99**, 12795 (2002).
- [2] J. Paulsson, *Nature (London)* **427**, 415 (2004).
- [3] N. G. Van Kampen, *Stochastic Processes in Physics and Chemistry* (North-Holland, Amsterdam, 1992).
- [4] T. G. Kurtz, *Math. Prog. Stud.* **5**, 67 (1976).
- [5] P. Hanggi, H. Grabert, P. Talkner, and H. Thomas, *Phys. Rev. A* **29**, 371 (1984).
- [6] F. Baras, M. M. Mansour, and J. E. Pearson, *J. Chem. Phys.* **105**, 8257 (1996).
- [7] M. Vellela and H. Qian, *J. R. Soc., Interface* **6**, 925 (2009).
- [8] P. S. Swain and A. Longtin, *Chaos* **16**, 026101 (2006).
- [9] A. A. Faisal, L. P. J. Selen, and D. M. Wolpert, *Nat. Rev. Neurosci.* **9**, 292 (2008).
- [10] W. R. Softky and C. Koch, *J. Neurosci.* **13**, 334 (1993).
- [11] K. Pakdaman, M. Thieullen, and G. Wainrib, *Adv. Appl. Probab.* **42**, 761 (2010).
- [12] D. Cai, L. Tao, M. Shelley, and D. W. McLaughlin, *Proc. Natl. Acad. Sci. U.S.A.* **101**, 7757 (2004).
- [13] A. V. Rangan, G. Kovacic, and D. Cai, *Phys. Rev. E* **77**, 041915 (2008).
- [14] D. Nykamp and D. Tranchina, *J. Comput. Neurosci.* **8**, 19 (2000).
- [15] A. Omurtag, B. W. Knight, and L. Sirovich, *J. Comput. Neurosci.* **8**, 51 (2000).
- [16] C. Ly and D. Tranchina, *Neural Comput.* **19**, 2032 (2007).
- [17] L. F. Abbott and C. van Vreeswijk, *Phys. Rev. E* **48**, 1483 (1993).
- [18] W. Gerstner and J. L. van Hemmen, *Phys. Rev. Lett.* **71**, 312 (1993).
- [19] N. Brunel and V. Hakim, *Neural Comput.* **11**, 1621 (1999).
- [20] N. Brunel, *J. Comput. Neurosci.* **8**, 183 (2000).
- [21] A. Renart, N. Brunel, and X.-J. Wang, in *Computational Neuroscience: A Comprehensive Approach* edited by J. Feng (CRC Press, Boca Raton, Florida, 2004) pp. 431–490.
- [22] C. Meyer and C. van Vreeswijk, *Neural Comput.* **14**, 369 (2002).
- [23] M. Mattia and P. Del Giudice, *Phys. Rev. E* **66**, 051917 (2002).
- [24] H. Soula and C. C. Chow, *Neural Comput.* **19**, 3262 (2007).
- [25] S. El Boustani and A. Destexhe, *Neural Comput.* **21**, 46 (2009).
- [26] B. Doiron, B. Lindner, A. Longtin, L. Maler, and J. Bastian, *Phys. Rev. Lett.* **93**, 048101 (2004).
- [27] M. J. Chacron, A. Longtin, and L. Maler, *Phys. Rev. E* **72**, 051917 (2005).
- [28] B. Lindner, B. Doiron, and A. Longtin, *Phys. Rev. E* **72**, 061919 (2005).
- [29] P. C. Bressloff, *SIAM J. Appl. Math.* **70**, 1488 (2009).
- [30] M. A. Buice and J. D. Cowan, *Phys. Rev. E* **75**, 051919 (2007).
- [31] M. Buice, J. D. Cowan, and C. C. Chow, *Neural Comput.* **22**, 377 (2010).
- [32] T. Ohira and J. D. Cowan, in *Proceedings of the First International Conference on Mathematics of Neural Networks* edited by S. Ellacott and I. J. Anderson (Academic, New York, 1997) pp. 290–294.
- [33] H. R. Wilson and J. D. Cowan, *Biophys. J.* **12**, 1 (1972).
- [34] H. R. Wilson and J. D. Cowan, *Kybernetik* **13**, 55 (1973).
- [35] M. I. Dykman, E. Mori, J. Ross, and P. M. Hunt, *J. Chem. Phys. A* **100**, 5735 (1994).
- [36] V. Elgart and A. Kamenev, *Phys. Rev. E* **70**, 041106 (2004).
- [37] R. Hinch and S. J. Chapman, *Eur. J. Appl. Math.* **16**, 427 (2005).
- [38] D. M. Roma, R. A. O’Flanagan, A. E. Ruckenstein, A. M. Sengupta, and R. Mukhopadhyay, *Phys. Rev. E* **71**, 011902 (2005).
- [39] C. Escudero and A. Kamenev, *Phys. Rev. E* **79**, 041149 (2009).
- [40] A. J. McKane, J. D. Nagy, T. J. Newman, and M. O. Stefanini, *J. Stat. Phys.* **128**, 165 (2007).
- [41] R. P. Boland, T. Galla, and A. J. McKane, *J. Stat. Mech.: Theory Exp.* (2008) P09001.
- [42] M. I. Freidlin and A. D. Wentzell, *Random Perturbations of Dynamical Systems* (Springer, New York, 1984).
- [43] R. S. Stein and D. L. Stein, *SIAM J. Appl. Math.* **57**, 752 (1997).
- [44] C. W. Gardiner, *Stochastic Methods: A Handbook for the Natural and Social Sciences*, 4th ed. (Springer, New York, 2009).
- [45] J. N. Teramae, H. Nakao, and G. B. Ermentrout, *Phys. Rev. Lett.* **102**, 194102 (2009).
- [46] H. G. Schuster and P. Wagner, *Biol. Cybern.* **64**, 77 (1990).
- [47] E. R. Grannan, D. Kleinfeld, and H. Sompolinsky, *Neural Comput.* **5**, 550 (1993).
- [48] A. Hutt, A. Longtin, and L. Schimansky-Geier, *Physica D* **237**, 755 (2008).
- [49] O. Faugeras, J. Touboul, and B. Cessac, *Frontiers in Comp., Neurosci.* **3**, 1 (2009).
- [50] R. Borisjuk and A. B. Kirillov, *Biol. Cybern.* **66**, 319 (1992).
- [51] P. G. Bolhuis, D. Chandler, C. Dellago, and P. L. Geissler, *Annu. Rev. Phys. Chem.* **53**, 291 (2002).
- [52] G. B. Ermentrout and J. D. Cowan, *Biol. Cybern.* **34**, 137 (1979).
- [53] G. B. Ermentrout, *Rep. Prog. Phys.* **61**, 353 (1998).
- [54] P. C. Bressloff, J. D. Cowan, M. Golubitsky, P. J. Thomas, and M. Wiener, *Philos. Trans. R. Soc. London, Ser. B* **356**, 299 (2001).
- [55] S. Coombes, *Biol. Cybern.* **93**, 91 (2005).
- [56] C. A. Lugo and A. J. McKane, *Phys. Rev. E* **78**, 051911 (2008).
- [57] J. M. Beggs and D. Plenz, *J. Neurosci.* **24**, 5216 (2004).
- [58] D. Plenz and T. C. Thiagarajan, *Trends Neurosci.* **30**, 101 (2007).
- [59] C. Bédard and A. Destexhe, *Biophys. J.* **96**, 2589 (2009).
- [60] R. Blake, *Brain and Mind* **2**, 5 (2001).
- [61] R. Blake and N. Logothetis, *Nat. Rev. Neurosci.* **3**, 13 (2002).
- [62] N. K. Logothetis, D. A. Leopold, and D. L. Sheinberg, *Nature (London)* **380**, 621 (1996).
- [63] S. R. Lehky, *Perception* **17**, 215 (1988).
- [64] S. R. Lehky, *Proc. R. Soc., London, Ser. B* **259**, 71 (1995).
- [65] R. Moreno-Bote, J. Rinzel, and N. Rubin, *J. Neurophysiol.* **98**, 1125 (2007).
- [66] A. Shpiro, R. Curtu, J. Rinzel, and N. Rubin, *J. Neurophysiol.* **97**, 462 (2007).
- [67] A. Shpiro, R. Moreno-Bote, N. Rubin, and J. Rinzel, *J. Comput. Neurosci.* **27**, 37 (2009).
- [68] C. R. Laing and C. C. Chow, *J. Comput. Neurosci.* **12**, 39 (2002).